μPMU-based islanding detection method in power distribution systems

Published Version:
Chafi, Z.S., Afrakhte, H., Borghetti, A. (2023). μPMU-based islanding detection method in power distribution systems. INTERNATIONAL JOURNAL OF ELECTRICAL POWER & ENERGY SYSTEMS, 151, 1-13 [10.1016/j.ijepes.2023.109102].

Availability:
This version is available at: https://hdl.handle.net/11585/928681 since: 2023-06-04

Published:
DOI: http://doi.org/10.1016/j.ijepes.2023.109102

μPMU-based Islanding Detection Method in Power Distribution Systems

Zahra Shafiei Chafi[a], Hossein Afrakhte[b]* ,Alberto Borghetti[c]

[a,b]*Department of Electrical Engineering, Faculty of Engineering, University of Guilan, P. O. Box 41996-13776, Rasht, Iran*
[c]*Department of Electrical, Electronic and Information Engineering, University of Bologna, viale Resiorgimento,2,40136 , Bologna, Italy*

Abstract

This paper focuses on the use of micro-phasor measurement units (μPMUs) for the prompt detection of unplanned islanding conditions. The investigated method is based on the monitoring of voltage and current phasors at distributed generation (DG) buses equipped by μPMUs. The difference between two consecutive phasors (voltage phasors and current phasors) are monitored until a perturbation occurs. When a perturbation is detected, the first phasor, called pre-disturbance phasor, is kept fixed and the second one, called post-disturbance phasor, is continuously updated with each new sample arrival. The differences between the pre-disturbance and post-disturbance phasors are calculated and summed up for a predefined time window. When this exceeds a predefined threshold, the island condition of the related bus is detected. The presented procedure can distinguish the islanding condition from other perturbations, such as motor starting, faults, and capacitor switching. The performance of the proposed procedure, as well as its sensitivity to the system conditions and predefined values, are analyzed considering a 7-bus distribution system and the IEEE 33-bus test system, both with synchronous generators and inverter-based DGs.

Keywords: Current measurements; Distribution system; Islanding detection; Micro-phasor measurement unit (μPMU); Voltage measurements

1. Introduction

1.1. Background

Unintentional islanding in distribution systems is the unplanned electrical disconnection of a part of the network with the connected loads and generators from the rest of the system. As the islanded system may operate without supervision, protection actions must be triggered to avoid serious dangers or specific control actions must be activated to maintain the safe and reliable operation. In both cases a prompt islanding condition detection is needed. Several approaches have been proposed in the literature (see e.g., [1] and reference therein).

The use of Phasor measurement units (PMUs) has led significant improvements in data collection, monitoring, and measurements in transmission systems. In power distribution systems, the use of PMUs is increasingly proposed and investigated for state estimation, monitoring, dynamic protection, and harmonic estimation. Due to the typical high precision and sampling rate of PMUs, several approached for their application also for islanding detection have been

* Hossein Afrakhte. Tel.: +981344083004; fax: +981316660070.
E-mail address: ho_afrakhte@guilan.ac.ir
http://dx.doi.org/10.1016/j.ijepes.2021.00.000

http://dx.doi.org/10.1016/j.ijepes.2021.000000

proposed [2-5].

PMUs used in transmission systems are not adequate to be applied in distribution systems, due to cost and much smaller phase angle difference between adjacent buses in distribution feeders than in the main grid. PMUs specifically designed for distribution systems, called μPMUs, have resolution and accuracy higher than conventional PMUs [6,7], as will be reviewed in Section 2.

1.2. Related works

Studies about the use of μPMUs for islanding detection are documented since 2018 [8], with several other contributions in the following years [6,9-11]. In [8] voltage and current phasors are obtained using fast Fourier transform (FFT) to be further processed by Fortescue transform. The absolute value of the difference between positive and zero components is used for islanding detection. In the approach proposed in [9], voltages at the busses with connected photovoltaic (PV) systems are monitored. Then, using Spectral Kurtosis and random forest classifier, three characteristics are extracted and applied for islanding detection. In [11], islands are detected using frequency and phase angle data obtained by μPMUs. The sum of the cumulative frequency difference and the phase angle difference are calculated, considering the linear relationship between them. Then the correlation between these two parameters is evaluated using Pearson correlation coefficient and the occurrence of the island is determined using a threshold value which is considered as a time band. In [10] a hybrid strategy is proposed that combines an active method, based on frequency shift slip mode as a positive feedback parameter using adaptive reactive power, with a remote method based on wide area measurements using μPMUs.

The method proposed in [10] appears only applicable for inverter based DGs and [6,9-11] have not been tested in a grid containing synchronous DGs. The methods proposed in [6, 8, 9] may require significant costly memory, since the calculations for islanding detection are performed at each DG bus instead of the control centre. Approaches proposed in [6,8] are characterized by long calculation procedures and the thresholds must be recalculated with the change of the grid topology. Because the method proposed in [9] is based on pattern recognition and intelligent separators, its performance depends on the comprehensiveness of the training data. If some characteristics of the system are not used for extracting the training data, the algorithm may not discriminate islanding events from other system disturbances. With the use of an active method, as in [10], there is the risk of weakening the power quality. Moreover, if the islanded system feeds only resistive load, reactive power injection may not cause the frequency drift needed to detect the islanding situation.

The important aspect of resilience in islanding detection is addressed in [9], although limited to generation outages, specifically PV units, without considering lines outages and the contribution of storage systems in supplying power after occurring an extreme outage event.

The limitations of the previously proposed approaches appear to motivate further studies in the development of improved islanding detection methods using μPMUs.

1.3. The novel contribution of the proposed method

In this paper a passive islanding detection method for distribution systems is described and its performance is analysed. The proposed approach uses μPMUs to collect voltage and current information over the network and uses some indices based on voltage and current phasors to detect islands. It uses the typical structure of μPMUs without any additional hardware change. The islanding condition is determined at each DG bus and the control centre is immediately informed. To increase the grid resilience in case of communication links interruptions, the calculated phasors are not sent to the control centre [9]. The calculations procedure is simple: it uses a two-level detecting principle and, as an improvement in reliability, two separated sets of measurements to distinguish islanding events from other disturbances. The threshold values for islanding detection are system dependent in some cases, but, in general, in this paper, there is no need to change or recalculate these values with the change of the grid topology. The proposed approach can be used in networks with different types of DGs (inverter based and synchronous generators). It has zero non detection zone (NDZ) and can distinguish the islanding event from non-islanding one within 6 cycles (0.12 seconds for 50 Hz systems and 0.1 seconds for 60 Hz systems), well within the 2 seconds maximum time limit according to IEEE 1547, IEC 62116, and UL 1741 standards.

Some of these characteristics represent an advantage with respect to those in practical use or presented in the literature. The use μPMUs without additional hardware change is particularly attractive when these devices are disseminated in the system for other purposes (e.g., monitoring and control).

The structure of the paper is as the following. The detailed description of the method is provided in Section 3. The considered test systems are described in Section 4 and the evaluation results are presented in Section 5. Section 6 is devoted to conclusions

2. Characteristics of the micro-PMUs

Table 1 compares the main characteristics of PMUs used in transmission systems and μPMUs. The accuracy of the measurements both in amplitude and phase angle in μPMUs are improved with respect to PMUs. Despite this superior performance, the cost of the μPMUs must be limited to have a wide application in distribution systems.

Table 1. Comparison between PMU and μPMU

Characteristic		PMU	μPMU
Measurement Accuracy [7, 12]	Amplitude (%F.S.)	0.1	0.010
	Phase (degree)	±0.5	±0.003
Cost ($/unit)		40000 to 180000 [13]	10000 [14]

μPMUs are expected to have higher resolution in comparison to PMUs used in the main grid, as distribution lines are typically much shorter than transmission lines, with a greater number of branches and electronic devices producing a significant signal to noise ratio (SNR), reduced power flows and phase angle differences at near busses.

The typical sampling rate in μPMUs is 30720 (for 60Hz frequency system) and 25600 (for 50Hz frequency system) [15]. This value is different from the reporting rate, which can be the same for both PMUs and μPMUs and it may be user selectable (for example, for 60 Hz systems, the typical reporting rate values are 10, 12, 15, 20, 30, 60 and 120 phasor estimates per second [16]).

3. Proposed method

This section presents the proposed islanding detection procedure based on voltage and current phasor estimates obtained by μPMUs installed in the distribution system at each DG bus.

3.1. Algorithm

The algorithm adopts a moving sum approach. Such an approach was also proposed for other detection purposes, e.g., for fault detection in [17] that describes an algorithm where the sum of current samples computed over one window cycle are compared with a threshold.

For the case of islanding detection, which may cause smaller changes in the current and voltage waveforms with respect to those due to the occurrence of faults, the moving sum approach is applied to the differences between a fixed pre-disturbance phasor and a variable post-disturbance one.

The algorithm starts by the sampling of voltage and current waveforms at each DG bus and by the phasor estimation of each μPMU (the phasor extraction procedure will be described in Section 3.2). Phasors are computed using a moving data window for the sampled voltage and current waveforms before and during the islanding event (as illustrated by Fig. 1). At each bus, one voltage measurement and different current measurements are available. As shown in Fig. 2, the developed procedure uses the voltage measured at the DG bus and the current measurements at the DG circuit breaker and at the termination of the line which connects the DG bus to the network.

The islanding instant is diagnosed using a moving data window. The moving data window moves forward with the arrival of each new sample. When this window contains the first perturbed sample, the algorithm is used to distinguish between a generic perturbance or an islanding condition.

During a pre-disturbance condition, the successive phasors do not change much with the introduction of new samples. When there is a perturbation, the voltage and current waveforms change suddenly. So, the computed phasors of these waveforms have different values in comparison to the phasors obtained before the perturbation occurrence. The perturbation causes a deviation between pre-disturbance phasors and the subsequent phasors. The differences between every two consecutive current and voltage phasors are monitored. When a perturbation occurs, the first phasor, called pre-disturbance phasor, is kept fixed and the second one called post-disturbance phasor, is continuously calculated with the arrival of each new sample and is subtracted from the first phasor. The sum of these differences is monitored and constantly updated for 6 cycles after the perturbation (0.1 s at 60 Hz and 0.12 s at 50Hz). If this sum exceeds the threshold value for both the voltage phasors at the DG bus and the current phasors at the terminal of the line that connects the DG bus to the network, then the occurring of the island is suspected. If the sum of the difference between current phasors at the DG circuit breaker also exceeds the threshold, the islanding condition of the DG bus is detected. Otherwise, the perturbation is a non-islanding event.

According to the described procedure, for DG bus *k* the difference between current phasors and between bus voltage phasors, are expressed as

$$IDF_k^i = \sum_{j=2}^{n} (I_k^{pre} - I_{kj}^{post}) \tag{1}$$

$$IDF_k^v = \sum_{j=2}^{n} (V_k^{pre} - V_{kj}^{post}) \tag{2}$$

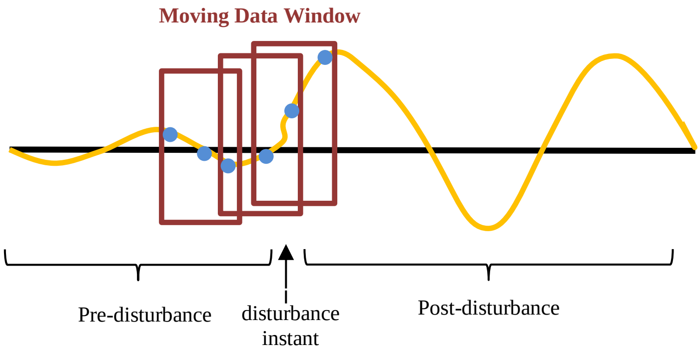

Fig. 1. Graphical representation of a typical voltage/current waveform showing the pre-disturbance and post-disturbance stages.

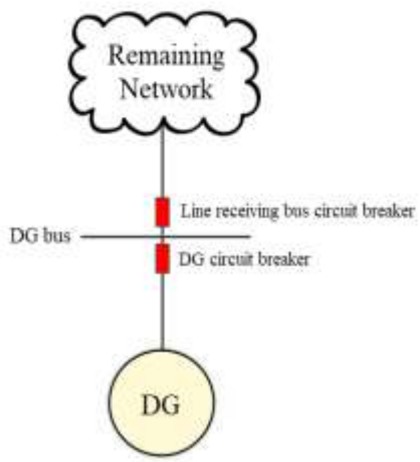

Fig. 2. Schematic diagram of a DG in the network.

where I_k^{pre} is the pre-disturbance current phasor, I_{kj}^{post} is the post-disturbance current phasor, V_k^{pre} is the pre-disturbance voltage phasor, and V_{kj}^{post} is the post disturbance voltage phasor. Counter j indicates the phasors that are continuously monitored for 6 cycles.

The current and the voltage phasors of all phases are monitored. The considered index for islanding detection is the average between the three phases (a, b, and c) for current and voltage measurements, respectively:

$$IDFF_k^i = \frac{1}{3}\left(\left|IDFF_k^{ia}\right| + \left|IDFF_k^{ib}\right| + \left|IDFF_k^{ic}\right|\right) \tag{3}$$

$$IDFF_k^v = \frac{1}{3}\left(\left|IDFF_k^{va}\right| + \left|IDFF_k^{vb}\right| + \left|IDFF_k^{vc}\right|\right) \tag{4}$$

Equation (3) is applied to the current phasor at the terminal of the line that connects the DG bus to the remaining grid and to the current phasor at the circuit braker of the DG.

By extending (3) and (4) to all DG buses in the network we have

$$\begin{bmatrix} (IDFF_1^i)_{Line} \\ IDFF_1^v \\ (IDFF_1^i)_{DG} \\ (IDFF_2^i)_{Line} \\ IDFF_2^v \\ (IDFF_2^i)_{DG} \\ \vdots \\ (IDFF_N^i)_{Line} \\ IDFF_N^v \\ (IDFF_N^i)_{DG} \end{bmatrix} \tag{5}$$

In (5) $IDFF_k^i$ has two different subscripts: subscript Line indicates the index calculated at the receiving termination of the connecting line; subscript DG indicates the index calculated at the DG circuit breaker. Every three consecutive rows of (5) are related to a different DG bus in the network. The indexes related to the first and the second row of each DG bus (i.e., the indexes for line current and voltage bus, respectively) are monitored and stored until they pass the threshold value. At this time also the third row (relevant to the DG current) is checked and if it exceeds the threshold the islanding condition is detected, otherwise the perturbation is not expected to be due to islanding.

Following the typical threshold selection procedure of [18,19], for the considered test cases, the values of the thresholds, i.e., the values that discriminate between islanding and non-islanding conditions, are chosen equal to 0.35 p.u. (called th_i) and 0.04 p.u. (called th_v).

3.2. Implementation

Time-domain voltage and current signals are sampled with high sampling rate (100kHz). The obtained waveforms are passed through a second order Butterworth filter with cut-off frequency of 350 Hz. In this way the waveforms high frequency harmonics are rejected. Next, the output of this filter is downsampled to 30720 Hz (512 samples per cycle), the typical sampling rate of a real μPMU. Then, the signals are passed through a least squares DC component removal filter. Finally, discrete Fourier transform (DFT) is deployed to extract the fundamental frequency component of the waveforms.

The flowchart of the proposed algorithm is shown in Fig. 3. The bus voltage and current measurements at DG

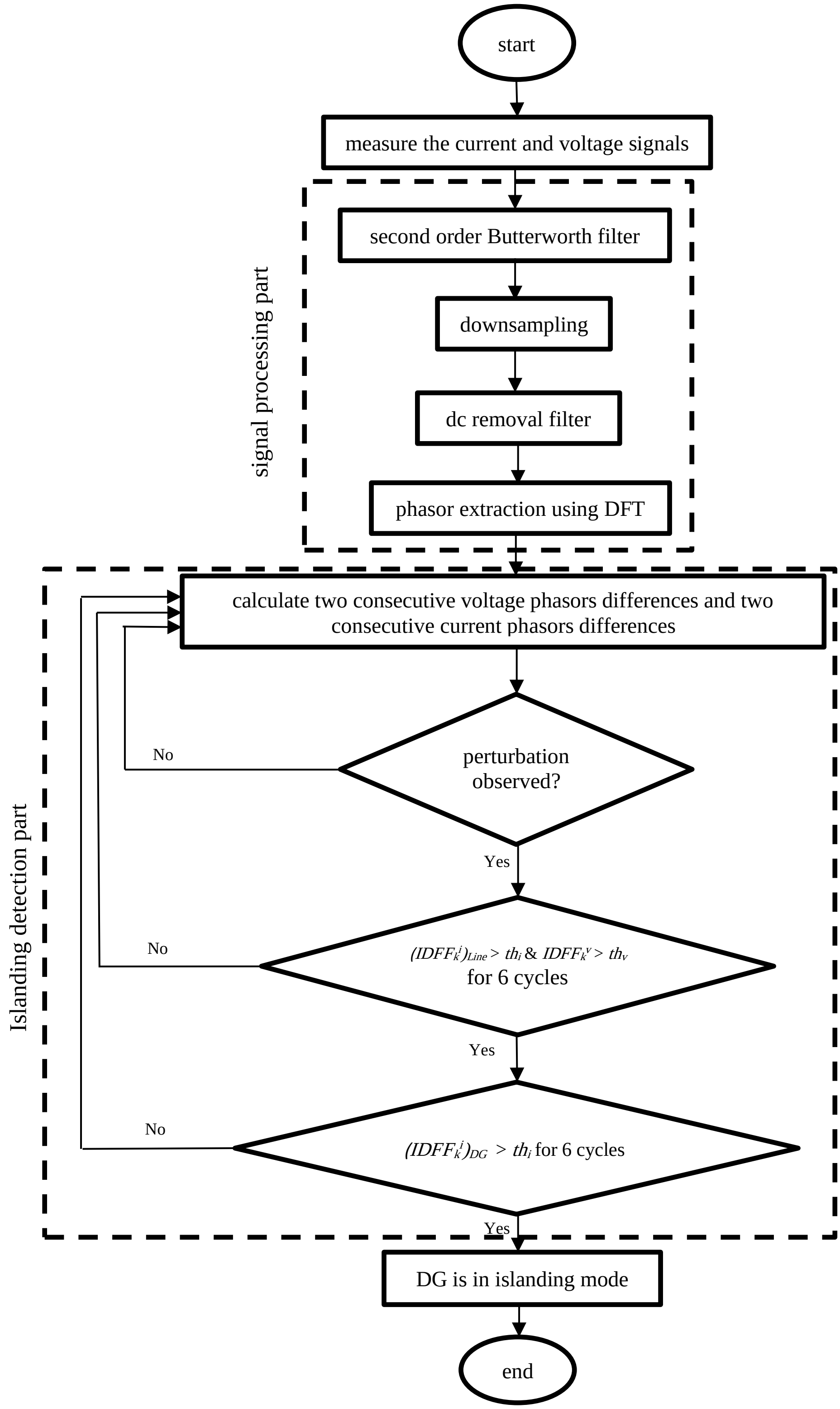

Fig. 3. Flowchart of the proposed method.

circuit breaker and at the terminal of the line that connects the DG bus to the remaining grid are used to extract the relevant phasor representation. After that, the islanding detection procedure is applied to the phasors. Initially, monitoring and calculation of the differences of the consecutive voltage and current phasors in the three phases are carried out separately. This monitoring is continued until a perturbation is detected. Then, the first phasor is kept fixed and the next one is updated repeatedly for 6 cycles. The sum of differences between these two phasors is monitored according to (3) and (4). If this difference exceeds the considered threshold for the sum of the voltage phasors and sum of the current phasors at the line terminal, then the cumulative difference relevant to the current phasors at the DG bus is checked. If it also exceeds the threshold, the islanding condition is detected, otherwise the monitoring of consecutive phasors is continued until a new perturbation occurs.

A perturbation is detected if the differences between two consecutive phasors of voltage or current in any phases exceeds a predefined value.

In the test cases considered in this paper, this value is chosen quite small (i.e., 10 - 5 p.u.). Obviously, the choice of the value is important to detect the perturbation and promptly start adding the differences between the phasors. If a too large value is chosen, the procedure may not activate or activate with a delay after the occurrence of the island condition, with the risk that the considered 6 cycles will not be sufficient to reach the threshold. If a too low value is chosen, the procedure is activated too often due to measurement errors or weak perturbations. This frequent activation of the procedure can obfuscate the detection of island conditions. In fact, if the procedure is unduly activated before the start of the island condition, the sum of the differences is terminated before the completion of the 6 cycles, with the risk that the threshold is not reached.

4. Test Systems

The proposed method has been assessed on two different test systems with radial configurations: a 7-bus test system and the IEEE 33-bus test system. The interface between DIgSILENT PowerFactory and MATLAB is used to represent the test systems and the proposed islanding detection approach, respectively. The test systems are represented in DIgSILENT that is used to simulate the considered transients. The resulting voltage and current signals are provided to MATLAB where the signal processing and islanding detection procedures are performed. The build in models of DIgSILENT software are used to represent inverter-based DGs controllers [20]. The results were obtained by using a computer with a 1.6 GHz core i5 processor and 4GB RAM. The computation time for the simulated cases is within half of a second.

4.1. 7-bus test system

The single-line diagram of the 7-bus system, adopted from [19], is shown in Fig. 4. It consists of 4 distribution lines, 3 DGs and 2 transformers. It is assumed that each DG bus is equipped with a μPMU. The modified system parameters with respect to [19] are reported in Table 2. Line 2 and line 3 have the same parameters of line 4. The lines are represented by their distributed parameter model. DG2 is a PV unit.

Table 2. 7-bus grid parameters.

Component	Value
L1	1.5+0.5j MVA
L2	0.6+0.3j MVA
L3	1+0.13j MVA
DG2	0.5 MVA

4.2. IEEE 33-bus test system

As it is shown in Fig. 5, the IEEE 33-bus test system [21] consists of 33 lines and 34 load points. It is assumed that 10% of the total load is connected at buses 13, 18, 24, 25 and 29 and the remaining 90% is connected to nodes 34 to

39, respectively [22]. The test system includes different types of DGs: two SG (synchronous generator), two PV and two DFIG (doubly fed injection generator) units are connected to nodes 34 to 39, as indicated in Table 3. The

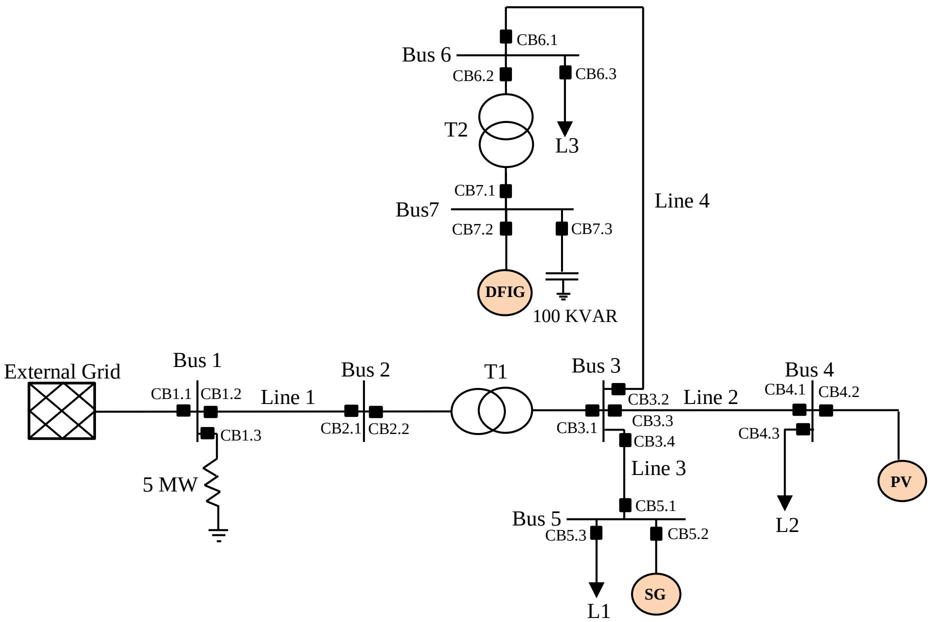

Fig. 4. Single line representation of 7-bus test system.

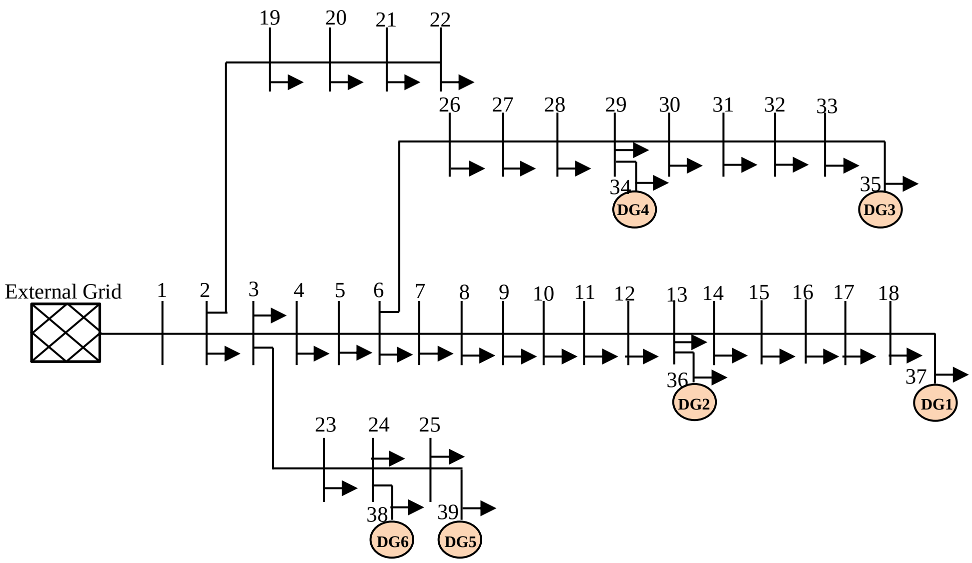

Fig. 5. IEEE 33-bus test system.

Table 3. IEEE 33-bus grid parameters.

Component	Type	Size (MW)
DG1	DFIG	1.6
DG2	SG	3.125
DG3	DFIG	1.6
DG4	PV	0.6
DG5	SG	3.125
DG6	PV	0.6

generators are connected to their corresponding buses through a CB.

5. Test Systems

5.1. 7-bus test system

Different islanding conditions (opening of the main circuit braker at the substation, separation of each DG bus) and non-islanding conditions (fault scenario, motor starting) are analysed. Moreover, the effects of load characteristics, power mismatch, capacitor switching, limited measurement accuracy, and data window size are investigated.

5.1.1 Tripping of the main CB

The main CB between the substation and bus1 is opened at 0 s. In this situation it is expected that all DGs detect that they are in islanding situation. The results are shown in Table 4.

According to Table 4, the values obtained at the end of the 6-cycle monitoring interval are larger than the corresponding threshold values, i.e., th_i = 0.35 p.u. and th_v = 0.04 p.u. (they are highlighted in the table). This confirms that all DGs detect the islanding condition.

Table 4. Tripping of the main CB (7-bus system).

Measuring point	$IDFF_K^i$ (Line)	$IDFF_K^i$ (DG)	$IDFF_k^v$
DFIG	1.8312	3.2106	0.8248
PV	0.4315	0.4428	0.9052
SG	4.5846	4.4031	0.6090

5.1.2 Islanding scenarios

The islanding scenario is caused by opening of the circuit breaker at the sending end of the lines that connect each DG bus to the network.

If line 2 is disconnected, the PV bus and its load is in islanding mode, as shown by the results in Table 5.

Table 5. Opening of line2 (7-bus system).

Measuring point	$IDFF_k^i$ (Line)	$IDFF_k^i$ (DG)	$IDFF_k^v$
DFIG	0.0245	---	0.0283
PV	0.6514	0.4423	1.1875
SG	0.1418	---	0.0221

If line 3 is disconnected, the SG bus is islanded, as shown in Table 6.

Table 6. Opening of line3 (7-bus system).

Measuring point	$IDFF_k^i$ (Line)	$IDFF_k^i$ (DG)	$IDFF_k^v$
DFIG	0.1472	---	0.0344
PV	0.0192	---	0.0442
SG	3.0656	3.4149	0.3628

The opening of the circuit breaker at the sending end of the line 4 causes the islanding of the DFIG bus, as shown in Table 7.

Table 7. Opening of line4 (7-bus system).

Measuring point	$IDFF_k^i$ (Line)	$IDFF_k^i$ (DG)	$IDFF_k^v$
DFIG	2.0604	2.0920	0.5858
PV	0.0207	---	0.0476
SG	0.3028	---	0.0293

5.1.3 Fault scenario

Different types of faults have been simulated at 0 s and considered to be cleared at 0.05 s. The results are shown in Fig. 6 to Fig. 9 (where the current measurements are obtained at the receiving bus of the line that connects each DG to the rest of the network) and in Table 8 and Table 9.

According to Table 8 and Table 9, for line to line to ground (LLG), line to line (LL), and single line to ground (SLG) faults the calculated indices do not reach the threshold values. But for the three phase (3PH) fault, the criterion related to the voltage for the SG bus exceeds the threshold. Since just one threshold is exceeded (the current criterion at the receiving end of the line that connects SG to the remaining network does not pass the threshold) SG bus is not in an islanding situation. The considered monitoring duration (0.1s) is longer than the duration that the fault exists in the grid. After the clearing time, the network backs to its normal state. As the calculation of the phasor differences is continued after clearing the fault, the small difference between subsequent phasors is added to the previous calculated phasor differences. This small difference decreases the total calculated average according to (3) and (4). In an islanding situation the deviation in signals will continue for the whole of the monitoring period. So, the summations (3) and (4) reach a significant value, larger than the thresholds.

In general, the primary line protection requires 3-4 cycles to clear the fault after relay has issued the trip command. However, sometimes faults persist for a longer duration (0.3-0.4 s) before being cleared by a backup protection. To evaluate the performance of the proposed method in this condition, different types of bolted faults have been simulated at 0 s and considered to be cleared at 0.350 s. In this case the fault exists for 21 cycles, longer than the monitoring interval adopted for evaluation of the islanding detection indices (6 cycles). As the algorithm is triggered by the perturbations (sufficient difference between two consecutive voltage or two consecutive current phasors), two perturbations will be observed: the first one at 0 s (i.e., at fault inception) and the second one at 0.350 s (i.e., at the fault clearing). The indexes will be calculated for 6 cycles after 0 s and for 6 cycles after 0.350 s.

The results for the first perturbation are the same as shown in Table 8 and Table 9. The results at the end of the 6 cycles interval after the second perturbation are shown in Table 10 and Table 11. For all types of the faults the proposed algorithm detects that the DGs are not in islanding mode.

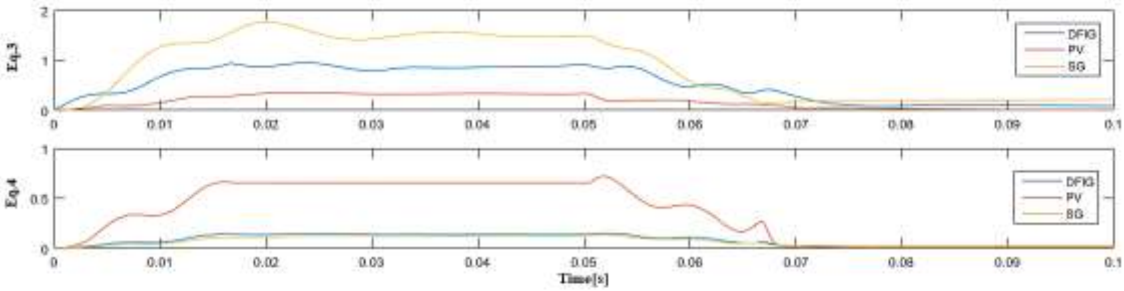

Fig. 6. Values of $IDFF_k^{\,v}$ and $IDFF_k^{\,i}$ after a LLG fault in line2 (7-bus system).

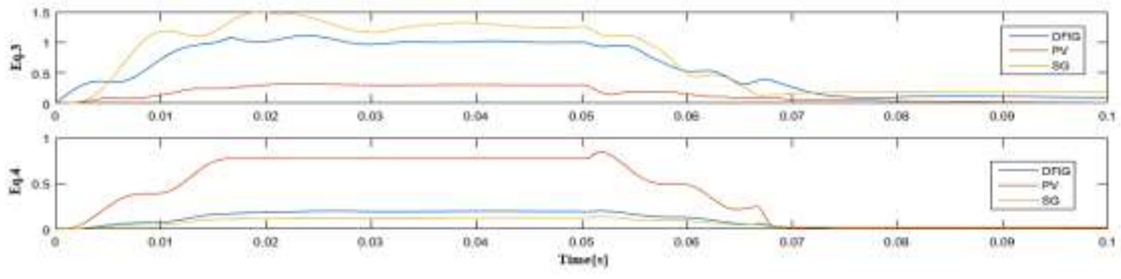

Fig. 7. Values of $IDFF_k^{\,v}$ and $IDFF_k^{\,i}$ after a LL fault in line 2 (7-bus system).

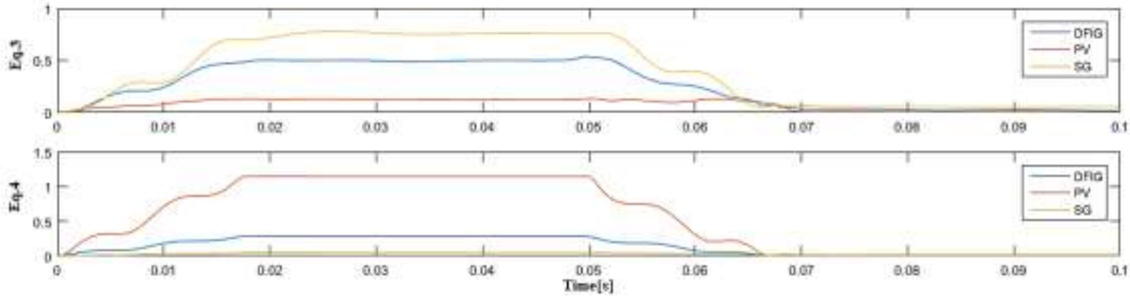

Fig. 8. Values of $IDFF_k^{\,v}$ and $IDFF_k^{\,i}$ after a SLG fault in line 2 (7-bus system).

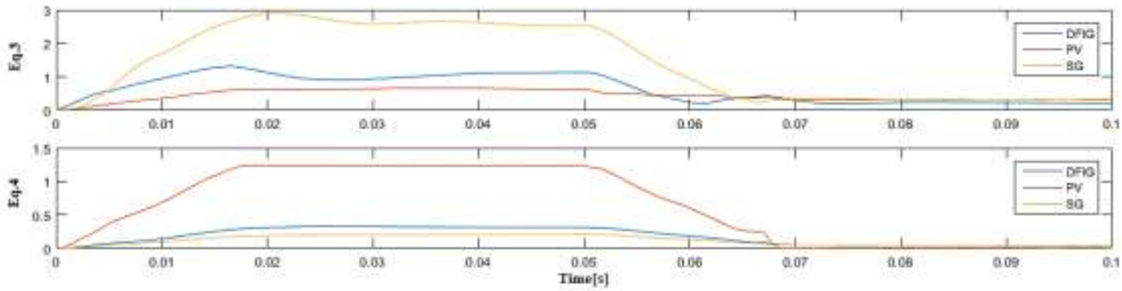

Fig. 9. Values of $IDFF_k^{\,v}$ and $IDFF_k^{\,i}$ after a 3PH fault in line 2 (7-bus system)

Table 8. Value of (3) at each DG bus for different types of faults in line 2 (7-bus system).

Fault type	point of evaluation of $IDFF_k^{\,i}$		
	CB6.1	CB4.1	CB5.1
LLG	0.0926	0.0080	0.2142
LL	0.0979	0.0092	0.1955
SLG	0.0164	0.0042	0.0578
3PH	0.2037	0.2562	0.3368

Table 9. Value of (4) at each DG bus for the different types of faults in line 2 (7-bus system).

Fault type	point of evaluation of $IDFF_k^{\,v}$		
	Bus6	Bus4	Bus5
LLG	0.0114	0.0122	0.0262
LL	0.0112	0.0118	0.0244
SLG	0.0114	0.0115	0.0151
3PH	0.0346	0.0079	0.0411

Table 10. Value of (3) at each DG bus for different types of faults in line 2 (7-bus system).

Fault type	point of evaluation of $IDFF_k^{\,i}$		
	CB6.1	CB4.1	CB5.1
LLG	0.2092	0.1288	0.4394
LL	0.2353	0.1255	0.4264
SLG	0.3192	0.2107	0.5712
3PH	0.2363	0.2267	0.2009

Table 11. Value of (4) at each DG bus for different types of faults in line 2 (7-bus system).

Fault type	point of evaluation of $IDFF_k^v$		
	Bus6	Bus4	Bus5
LLG	0.0570	0.2415	0.0305
LL	0.0406	0.1829	0.0301
SLG	0.1304	0.5856	0.0293
3PH	0.0701	0.9434	0.0184

5.1.4 Motor starting (nonlinear load effect)

To evaluate the performance of the proposed algorithm during the start of induction motors, an increasing number of motors (1, 4, 8 and 10, with total rated power of 100 kW, 400 kW, 800 kW, and 1000 kW, respectively) are simultaneously started at bus 3. Motors parameters are reported in [18]. Table 12 and Table 13 summarizes the results.

According to Table 12 and Table 13, the value of indexes (3) and (4) for each DG bus increases with the increase of the number of simultaneously started motors. The values for 1 motor, 4 motors and 8 motors are less than the considered thresholds. For the case 10 motors the threshold value related to the voltage at the PV unit is crossed. As just one criterion is met the proposed method recognizes that the PV bus is not in islanding mode.

Table 12. Value of (3) at each DG bus during motor starting (7-bus system).

point of evaluation of $IDFF_k^i$	1 motor	4 motors	8 motors	10 motors
CB6.1	0.0146	0.0572	0.1135	0.1411
CB4.1	0.0027	0.0068	0.0122	0.0148
CB5.1	0.0276	0.1270	0.2544	0.3160

Table 13. Value of (4) at each DG bus during motor starting (7-bus system).

point of evaluation of $IDFF_k^v$	1 motor	4 motors	8 motors	10 motors
Bus6	0.0052	0.0157	0.0308	0.0383
Bus4	0.0058	0.0194	0.0380	0.0472
Bus5	0.0049	0.0113	0.0209	0.0257

5.1.5 Load modelling effect

To analyse the effect of load modelling on the accuracy of the proposed islanding detection algorithm, for all the loads, the PQ model is replaced by the voltage dependent model:

$$P_L = P_0(aP(\frac{V}{V_0})^{n1} + bP(\frac{V}{V_0})^{n2} + (1 - aP - bP)(\frac{V}{V_0})^{n3}) \quad (6)$$

$$Q_L = Q_0(cQ(\frac{V}{V_0})^{m1} + dQ(\frac{V}{V_0})^{m2} + (1 - cQ - dQ)(\frac{V}{V_0})^{m3}) \quad (7)$$

where P_0 and Q_0 are the initial operating conditions, V_0 is the rated voltage value, and aP, bP, cQ, dQ, $n1$, $n2$, $n3$, $m1$, $m2$ and $m3$ are parameters with values adopted from Table 14. The results of the indices shown in Table 15 and Table 16 confirm that each islanding condition which is caused by the opening of the CB at the sending bus that connects the bus to the remaining network is correctly detected.

According to Table 15 and Table 16 the change of the load type has not affected the accuracy of the algorithm and the islanding conditions are correctly detected (as in other tables, the values that exceed the threshold are highlighted).

Table 14. Voltage dependent load parameters.

	Parameters									
	aP	bP	cQ	dQ	n1	n2	n3	m1	m2	m3
P_L	0.7	0.2	---	---	0	1	2	---	---	---
Q_L	---	---	0.95	0.05	---	---	---	0	1	2

Table 15. Value of (3) at each DG bus for voltage dependent load scenario (7-bus system).

islanding	point of evaluation of $IDFF_k^i$					
	Bus5 (Line)	at the terminal of SG	Bus6 (Line)	at the terminal of DFIG	Bus4 (Line)	at the terminal of PV
DFIG	0.3066	---	2.0650	2.1937	0.0233	---
PV	0.0634	---	0.0293	---	0.5864	0.4223
SG	1.9486	1.7471	0.0384	---	0.0074	---

Table 16. Value of (4) at each DG bus for voltage dependent load scenario (7-bus system).

islanding	point of evaluation of $IDFF_k^v$		
	Bus5	Bus6	Bus4
DFIG	0.0265	0.5518	0.0450
PV	0.0041	0.0069	1.2359
SG	0.2956	0.0156	0.0178

5.1.6 Power mismatch effect

The power mismatch is defined as the power being lost in terms of percentage of the total load just before islanding. Active and reactive power mismatches are the critical factors for the maloperation of many conventional techniques. According to IEEE-1547, islanding detection should be tested for various active power and reactive power mismatches. This subsection considers the worst case, i.e., the islanding at zero power mismatch. Moreover, also for 5% active and reactive power mismatch conditions, the results confirm the adequacy of the proposed method. For all cases, the islanding situation is caused by the opening of the main CB at bus 1.

To apply a 0% and 5% active power mismatch, the loads are changed with a correction factor. The results shown in Table 17 and Table 18 confirm that the islanding situation is detected as all the obtained values exceed the threshold values.

Table 17. Value of (3) at each DG bus for active power mismatch scenario (7-bus system).

active power mismatch value(%)	point of evaluation of $IDFF_k^i$					
	Bus5 (Line)	at the terminal of SG	Bus6 (Line)	at the terminal of DFIG	Bus4 (Line)	at the terminal of PV
0	4.3239	4.1513	1.9957	2.4714	0.3775	0.4079
5	4.3361	4.1640	1.9985	2.4810	0.3791	0.4080

Table 18. Value of (4) at each DG bus for active power mismatch scenario (7-bus system).

active power mismatch value (%)	point of evaluation of $IDFF_k^v$		
	Bus5	Bus6	Bus4
0	0.4588	0.6535	0.7332
5	0.4616	0.6597	0.7368

For the representation of active power mismatch, the load at bus 2 is changed to reach the desired percentage of the reactive power (0% and 5%). The results reflected in Table 19 and Table 20 reveal that reactive power mismatch does not affect the performance of the proposed algorithm.

Table 19. Value of (3) at each DG bus for reactive power mismatch scenario (7-bus system).

reactive power mismatch value(%)	point of evaluation of $IDFF_k^i$					
	Bus5 (Line)	at the terminal of SG	Bus6 (Line)	at the terminal of DFIG	Bus4 (Line)	at the terminal of PV
0	5.2918	5.3782	2.0513	2.6669	0.4661	0.4771
5	5.2584	5.3449	2.0454	2.6624	0.4447	0.4725

Table 20. Value of (4) at each DG bus for reactive power mismatch scenario (7-bus system).

reactive power mismatch value (%)	point of evaluation of $IDFF_k{}^v$		
	Bus5	Bus6	Bus4
0	0.6978	0.9548	1.0419
5	0.6323	0.8672	1.0036

5.1.7 Effect of capacitor switching

To evaluate the ability of the proposed method in distinguishing the islanding conditions from capacitor switching, a 1.5 Mvar capacitor is assumed to be connected to bus 3 at 0 s (analogous results are obtained for connecting to different buses or different size of the capacitor bank). The results of Table 21 show that the obtained values of the indices are lower than the threshold values, so the method identifies that there is no islanding situation.

Table 21. Capacitor switching (7-bus system).

Measuring point	$IDFF_k^i$	$IDFF_k{}^v$
DFIG	0.1020	0.0256
PV	0.0133	0.0320
SG	0.1736	0.0232

5.1.8 Effect of erroneous measurements

Small errors in magnitude and phase angle have been introduced in the μPMUs estimates at SG bus (bus 5), DFIG bus (bus 6) and PV bus (bus 4). The islanding event of each DG under these conditions has been analysed.

The obtained measurements at SG bus, DFIG bus and PV bus have 1, 2 and 3 percent error in magnitude for current and voltage measurements, respectively. The obtained measurements at SG bus, DFIG bus and PV bus have 1, 2 and 3 degree error in phase angle for current and voltage signals, respectively. The islanding of each DG is due to the opening of the CB that connects each DG bus to the remaining network. The results are shown in Table 22 to Table 24. The erroneous measurements do not affect the accuracy of the proposed method and the results show that the occurrence of the island is appropriately detected in all cases.

5.1.9 Effect of data window size

Small errors in A longer window with respect to the adopted 6-cycle monitoring interval, increases the accuracy but decreases the response time and process speed. To assess the difference in the performances, the signal is sampled with the rates equal to 384 and 1024 samples per cycle (different from the rate used for other simulations, i.e., 512 samples per cycle).

The results are shown in Table 25 to Table 28. According to the results, the capability of the proposed approach to detect the islanding conditions is not significantly affected by the sampling rate and the window size.

Table 22. Values of (3) at each DG bus for erroneous measurements scenario for islanding of SG and PV (7-bus system).

Measurement error	Erroneous measurement position	Erroneous measurement type	Islanding of SG				Islanding of PV			
			point of evaluation of $IDFF_k^i$				point of evaluation of $IDFF_k^i$			
			Bus5 (Line)	at the terminal of SG	Bus4 (Line)	Bus6 (Line)	Bus5 (Line)	Bus4 (Line)	at the terminal of PV	Bus6 (Line)
1% in magnitude	bus 5	voltage	1.8596	1.6790	0.0057	0.0360	0.0567	0.4998	0.4202	0.0235
		current	1.8782	1.6790	0.0057	0.0360	0.0573	0.4998	0.4202	0.0235
1° in phase angle	bus 5	voltage	1.8596	1.6790	0.0057	0.0360	0.0567	0.4998	0.4202	0.0235
		current	1.8686	1.6790	0.0057	0.0360	0.0566	0.4998	0.4202	0.0235
2% in magnitude	bus 6	voltage	1.8596	1.6790	0.0057	0.0360	0.0567	0.4998	0.4202	0.0235
		current	1.8596	1.6790	0.0057	0.0367	0.0567	0.4998	0.4202	0.0239
2° in phase angle	bus 6	voltage	1.8596	1.6790	0.0057	0.0360	0.0567	0.4998	0.4202	0.0235
		current	1.8596	1.6790	0.0057	0.0361	0.0567	0.4998	0.4202	0.0236
3% in magnitude	bus 4	voltage	1.8596	1.6790	0.0057	0.0360	0.0567	0.4998	0.4202	0.0235
		current	1.8596	1.6790	0.0059	0.0360	0.0567	0.5148	0.4202	0.0235
3° in phase angle	bus 4	voltage	1.8596	1.6790	0.0057	0.0360	0.0567	0.4998	0.4202	0.0235
		current	1.8596	1.6790	0.0057	0.0360	0.0567	0.5002	0.4202	0.0235

Table 23. Values of (3) at each DG bus for erroneous measurements scenario for islanding of DFIG (7-bus system).

Measurement error	Erroneous measurement position	Erroneous measurement type	Islanding of DFIG			
			point of evaluation of $IDFF_k^i$			
			Bus5 (Line)	Bus4 (Line)	Bus6 (Line)	at the terminal of DFIG
1% in magnitude	bus 5	voltage	0.2962	0.0195	2.0199	2.1478
		current	0.2991	0.0195	2.0199	2.1478
1° in phase angle	bus 5	voltage	0.2962	0.0195	2.0199	2.1478
		current	0.2959	0.0195	2.0199	2.1478
2% in magnitude	bus 6	voltage	0.2962	0.0195	2.0199	2.1478
		current	0.2962	0.0195	2.0603	2.1478
2° in phase angle	bus 6	voltage	0.2962	0.0195	2.0199	2.1478
		current	0.2962	0.0195	2.0369	2.1478
3% in magnitude	bus 4	voltage	0.2962	0.0195	2.0199	2.1478
		current	0.2962	0.0201	2.0199	2.1478
3° in phase angle	bus 4	voltage	0.2962	0.0195	2.0199	2.1478
		current	0.2962	0.0193	2.0199	2.1478

Table 24. Value of (4) at each DG bus for erroneous measurements scenario (7-bus system).

Measurement error	Erroneous measurement position	Erroneous measurement type	Islanding of SG			Islanding of PV			Islanding of DFIG		
			point of evaluation of $IDFF_k^v$			point of evaluation of $IDFF_k^v$			point of evaluation of $IDFF_k^v$		
			Bus5	Bus4	Bus6	Bus5	Bus4	Bus6	Bus5	Bus4	Bus6
1% in magnitude	bus 5	voltage	0.2870	0.0165	0.0143	0.0043	1.2436	0.0067	0.0247	0.0433	0.5842
		current	0.2842	0.0165	0.0143	0.0042	1.2436	0.0067	0.0244	0.0433	0.5842
1° in phase angle	bus 5	voltage	0.2853	0.0165	0.0143	0.0042	1.2436	0.0067	0.0244	0.0433	0.5842
		current	0.2842	0.0165	0.0143	0.0042	1.2436	0.0067	0.0244	0.0433	0.5842
2% in magnitude	bus 6	voltage	0.2842	0.0165	0.0146	0.0042	1.2436	0.0069	0.0244	0.0433	0.5959
		current	0.2842	0.0165	0.0143	0.0042	1.2436	0.0067	0.0244	0.0433	0.5842
2° in phase angle	bus 6	voltage	0.2842	0.0165	0.0143	0.0042	1.2436	0.0067	0.0244	0.0433	0.5871
		current	0.2842	0.0165	0.0143	0.0042	1.2436	0.0067	0.0244	0.0433	0.5842
3% in magnitude	bus 4	voltage	0.2842	0.0170	0.0143	0.0042	1.2809	0.0067	0.0244	0.0446	0.5842
		current	0.2842	0.0165	0.0143	0.0042	1.2436	0.0067	0.0244	0.0433	0.5842
3° in phase angle	bus 4	voltage	0.2842	0.0164	0.0143	0.0042	1.2478	0.0067	0.0244	0.0432	0.5842
		current	0.2842	0.0165	0.0143	0.0042	1.2436	0.0067	0.0244	0.0433	0.5842

Table 25. Value of (3) at each DG bus for each islanding scenario with the sampling rate of 384 sample/cycle (7-bus system).

islanding	point of evaluation of $IDFF_k^i$					
	Bus5 (Line)	at the terminal of SG	Bus6 (Line)	at the terminal of DFIG	Bus4 (Line)	at the terminal of PV
DFIG	0.2963	---	2.0204	2.1503	0.0195	---
PV	0.0567	---	0.0265	---	0.4998	0.4202
SG	1.8600	1.6794	0.0401	---	0.0057	---

Table 26. Value of (4) at each DG bus for each islanding scenario with the sampling rate of 384 sample/cycle (7-bus system).

islanding	point of evaluation of $IDFF_k^v$		
	Bus5	Bus6	Bus4
DFIG	0.0245	0.5842	0.0434
PV	0.0043	0.0070	1.2436
SG	0.2842	0.0140	0.0164

Table 27. Value of (3) at each DG bus for each islanding scenario with the sampling rate of 1024 sample/cycle (7-bus system).

islanding	point of evaluation of $IDFF_k^i$					
	Bus5 (Line)	at the terminal of SG	Bus6 (Line)	at the terminal of DFIG	Bus4 (Line)	at the terminal of PV
DFIG	0.4366	---	3.2658	3.1934	0.0338	---
PV	0.1007	---	0.0382	---	0.7934	0.6709
SG	3.0089	2.7939	0.0764	---	0.0083	---

Table 28. Value of (4) at each DG bus for each islanding scenario with the sampling rate of 1024 sample/cycle. (7-bus system)

islanding	point of evaluation of $IDFF_k^v$		
	Bus5	Bus6	Bus4
DFIG	0.0378	0.8133	0.0684
PV	0.0081	0.0111	2.1135
SG	0.2963	0.0204	0.0254

5.2 IEEE 33-bus test system

To evaluate the ability The performances of the proposed islanding detection method are confirmed by the results obtained for the IEEE 33-bus test system. Different islanding conditions have been simulated and the results of islanding of each DG separately are shown in Table 29 and Table 30. In these tables the islanding of DG2, DG4 and DG6 are caused by opening of the CB that connects each DG to the corresponding DG bus. After the separation, these DGs continue feeding their local load.

The results relevant to the islanding of all DGs by opening of the main CB are shown in Table 31.

The results related to separate islanding of DG1 and DG2, DG3 and DG4, DG5 and DG6 are presented in Table 32, Table 33 and Table 34, respectively.

According to all these results, the proposed method retains its performance in all different islanding scenarios.

6. Reliability Assessment of the Proposed Method

The proposed islanding detection method for systems reflected in Fig. 4 and Fig. 5 is called reliable if it detects all DGs situation true (island or not). Furthermore, it detects each DG is in island or not truly. If it detects only one DG's situation mistakenly it is not reliable. Although in the stated sentence, the reliability is considered qualitatively, but it is possible to define an index for that. Therefore, the islanding detection reliability index for 7-bus test system can be expressed as (8) and (9) and for IEEE 33-bus test system can be expressed as (10) and (11):

Table 29. Values of (3) at each DG bus for the islanding scenarios (IEEE 33-bus system).

CB opening	point of evaluation of $IDFF_k^i$											
	Bus18	at the terminal of DG1	Bus13	at the terminal of DG2	Bus33	at the terminal of DG3	Bus29	at the terminal of DG4	Bus25	at the terminal of DG5	Bus24	at the terminal of DG6
Bus18 (DG)	0.5608	0.3602	0.3430	---	0.0295	---	0.5851	0.0900	4.9220	---	0.3082	---
Bus13 (DG)	0.2695	---	1.0012	1.2997	0.0653	---	0.0850	---	0.0463	---	0.0414	---
Bus33 (DG)	0.0515	---	0.0550	---	1.1622	2.0086	0.0159	---	0.2534	---	3.2287	---
Bus29 (DG)	0.0187	---	0.0197	---	0.0178	---	0.5741	1.3039	0.0758	---	0.0959	---
Bus25 (DG)	0.0052	---	0.0046	---	0.0402	---	0.0278	---	3.1020	1.0477	0.0152	---
Bus24 (DG)	0.0115	---	0.0133	---	0.0149	---	0.0266	---	0.0693	---	1.9493	0.9388

Table 30. Value of (4) at each DG bus for the islanding scenarios (IEEE 33-bus system).

CB opening	point of evaluation of $IDFF_k^v$					
	Bus18	Bus13	Bus33	Bus29	Bus25	Bus24
Bus18(DG)	0.1273	0.0736	0.0009	0.5976	0.0290	0.0136
Bus13(DG)	0.0333	0.0422	0.0114	0.0119	0.0187	0.0187
Bus33(DG)	1.1519	0.0608	0.1257	0.0041	0.0287	0.0136
Bus29(DG)	0.0671	0.0507	0.3504	0.2494	0.0177	0.0084
Bus25(DG)	0.0160	3.4380	0.0005	0.0341	0.0673	0.0182
Bus24(DG)	0.0133	0.0572	0.0045	0.0134	0.0145	0.4062

Table 31. Values of (3) and (4) at each DG bus after opening of MCB (IEEE 33-bus system).

Measuring Point	$IDFF_k^i$ (Line)	$IDFF_k^i$ (DG)	$IDFF_k^v$
Bus18	1.1859	0.9184	0.6846
Bus13	5.1191	3.7009	0.7193
Bus33	2.1019	1.2332	0.9126
Bus29	2.3302	0.4919	0.9267
Bus25	3.1969	2.2644	1.0138
Bus24	3.6976	0.4746	1.0260

Table 32. Values of (3) and (4) at each DG bus after opening of line 6-7 (IEEE 33-bus system).

Measuring point	$IDFF_k^i$ (Line)	$IDFF_k^i$ (DG)	$IDFF_k^v$
Bus18	1.7591	0.8706	0.7015
Bus13	7.1580	5.0451	0.7613
Bus33	0.2778	---	0.1071
Bus29	0.3301	---	0.1100
Bus25	0.2031	---	0.224
Bus24	0.1893	---	0.0208

Table 33. Values of (3) and (4) at each DG bus after opening of line 26-27 (IEEE 33-bus system).

Measuring point	$IDFF_k^{\,i}$ (Line)	$IDFF_k^{\,i}$ (DG)	$IDFF_k^{\,v}$
Bus18	0.0523	---	0.0338
Bus13	0.3405	---	0.0357
Bus33	2.3124	0.8279	0.6315
Bus29	2.7035	0.6554	0.6685
Bus25	0.0945	---	0.0196
Bus24	0.1007	---	0.0200

Table 34. Values of (3) and (4) at each DG bus after opening of line 3-23 (IEEE 33-bus system).

Measuring point	$IDFF_k^{\,i}$ (Line)	$IDFF_k^{\,i}$ (DG)	$IDFF_k^{\,v}$
Bus18	0.0036	---	0.0009
Bus13	0.1324	---	0.0010
Bus33	0.0172	---	0.0044
Bus29	0.0206	---	0.0047
Bus25	4.7626	3.6924	0.9917
Bus24	5.400	0.4486	1.0229

$$R_{event}=p^3 \tag{8}$$
$$Q_{event}=3p^2q+3pq^2+q^3 \tag{9}$$

$$R_{event}=p^6 \tag{10}$$
$$Q_{event}=6p^5q+15p^4q^2+20p^3q^3+15p^2q^4+6pq^5+q^6 \tag{11}$$

where p is the probability of correctly detect a DG's situation (in fact the probability of exceeding the threshold for islanded DG or not exceeding the threshold for non-islanded DG) and q is the fail in correctly detect island (it is assumed that the probability of successfully detect islands for all DGs has the same value). R_{event} and Q_{event} are the reliability of the method for the system and the unreliability of the method for the system, respectively. According to (8) and (10) the islanding detection method is reliable if all DGs' situation diagnosed truly.

In order to assess the reliability of the proposed method, three other situations are defined: only one group of measurement is used ($IDFF_k^{\,v}$ or $IDFF_k^{\,i}$ (Line)) and one level islanding detection principle ($IDFF_k^{\,v}$ & $IDFF_k^{\,i}$ (Line)) is considered. The results for some previous simulated events are reflected in Table 35 (S: successfully detect the situation of DGs, F: fail in detecting the situation of DG(s) which are highlighted). For each criterion and each event if the method detects all DGs' situation true, the method is successful in detecting the DG's situation in the system and is addressed with 'S' also if the method detects the DGs' situation mistakenly (one of them or more), the method fails in detecting the DG's situation in the system and is addressed with 'F'. For example, according to Table 6 and considering the criterion $IDFF_k^{\,v}$, it exceeds the threshold for SG and for DFIG it does not pass the threshold but for PV which is not in islanding situation it detects that it is islanded. So, this criterion fails in detecting the DGs' situations in the system.

It can be seen that only the proposed method can detect all DGs' situation successfully. The reliability of each islanding detection criterion for the system can be calculated using (8) for 7-bus system (columns 2 to 10) and (10) (columns 11 to 13) for cases has the result "S". For example, with assuming the probability of detecting correctly the DGs' situations equal to 0.98, the reliability for 7 bus system is 0.9412 and for 33-bus system is 0.8858.

Table 35. The operating condition of different indices in islanding detection.

Islanding detection criterion (criteria)	Event (Table Numbers)											
	6	7	8 & 9 (3PH fault)	10 & 11 (3PH fault)	10 & 11 (LLG fault)	10 & 11 (LL fault)	10 & 11 (SLG fault)	12 & 13 (10 motors)	15 & 16	27 & 28	29 & 30	32
	Detecting island	Detecting island	Detecting island	Detecting island	Detecting island	Detecting island	Detecting island	Detecting island	Detecting island	Detecting island	Detecting island	Detecting island
$IDFF_k^{\ v}$	F	F	F	F	F	F	F	F	F	F	F	F
$IDFF_k^{i}$ (Line)	S	S	S	S	F	F	F	S	S	S	F	S
$IDFF_k^{\ v}$ & $IDFF_k^{i}$ (Line)	S	S	S	S	S	S	S	S	S	S	F	S
Proposed Method	S	S	S	S	S	S	S	S	S	S	S	S

7. Conclusion

Early islanding detection is useful to activate protections against unwanted islands or to activate suitable control modes able to support the islanding operation. There is a general tendency to install μPMUs in distribution networks for both protection and control purposes. In this paper a novel islanding detection scheme based on monitoring the current and voltage phasors obtained by μPMUs installed at each DG bus is presented. Consecutive current and consecutive voltage phasors are monitored until a disturbance occurs. The voltage phasor is estimated at the DG bus and the current phasor is estimated at the receiving end of the line that connects the DG to the remaining network. The difference between consecutive current and consecutive voltage phasors are monitored until a disturbance occurs. In the normal operation these differences are nearly zero. When a perturbation happens, they have a nonzero value. At this time, the first phasor is kept fixed, the other phasor is constantly updated with the arrival of each new sample. The cumulative sum of these differences is calculated for 6 cycles and, if this value exceeds the threshold, then an islanding situation may present. To confirm this, the sum of this difference is checked also for the current phasors estimated at the DG circuit breaker. If also this value passes the threshold, the islanding condition is detected.

The proposed method is validated by a 7-bus system and the IEEE 33-bus test feeder. Various scenarios, such as the islanding of each DG bus, different types of faults, capacitor switching, trip of the main circuit breaker, switching of different number of induction motors are represented and the effect of load modelling, data window size, and erroneous measurements are considered.

The tests show that the proposed method can differentiate between islanding and non-islanding events. Furthermore, the proposed method can detect the islanding conditions with zero NDZ within 0.1 s for 60 Hz and 0.12 s for 50 Hz systems, well below than the maximum time (2 seconds) reported in IEEE1547, UL 1741, and IEC 62116 standards.

There are some issues that may affect the performance of the proposed method including high penetration of electric vehicles or storage systems. This may enforce transients behave similar to islanding event. Occurring two or more simultaneous events in different parts of the network in which at least one is islanding is another concern that may impress the performance of the proposed method.

Future work will devote to observe these cases. The first case may be solved by adding another part that use machine learning or fuzzy logic based algorithms to diagnose these special kinds of signals and discriminate them from islanding events. The second case may be solved by adding other indexes calculating in parallel with each other for each event or add calculating parts similar to the proposed method that have different data window size.

References

[1] M.S. Kim, R. Haider, G-J. Cho, C-H. Kim, C-Y. Won, and J-S. Chai, "Comprehensive review of islanding detection methods for distributed generation systems," Energies, vol. 12, no. 5, p. 837, Feb. 2019.

[2] M.M. Ostojić, and M.B. Djurić, "The algorithm with synchronized voltage inputs for islanding detection of synchronous generators," Int. Journal of Elec. Power & Energy Syst, vol. 103, pp. 431-439, Dec. 2018.

[3] D. Sivadas and K. Vasudevan, "An active islanding detection strategy with zero nondetection zone for operation in single and multiple inverter mode using GPS synchronized pattern," IEEE Trans. on Indust. Elect., vol. 67, no. 7, pp. 5554-5564, July 2020.

[4] Y. Guo, K. Li, D. M. Laverty and Y. Xue, "Synchrophasor-based islanding detection for distributed generation systems using systematic principal component analysis approaches," IEEE Trans. on Power Del., vol. 30, no. 6, pp. 2544-2552, Dec. 2015.

[5] A. Sankar and R. Sunitha, "Synchrophasor data driven islanding detection, localization and prediction for microgrid using energy operator," in IEEE Trans. on Power Syst., vol. 36, no. 5, pp. 4052-4065, Sep. 2021.

[6] A. Shukla, S. Dutta, and P.K. Sadhu, "An island detection approach by μ-PMU with reduced chances of cyber-attack," Int. Journal of Elect. Power & Energy Syst., vol. 126, p. 106599, March 2021.

[7] "Data Sheet micro-PMU Features", Power Standards Lab Inc., Nov. 2018, Available: https://pdf.directindustry.com/pdf/power-standards-lab/micropmu/207207-856169.html

[8] S. Dutta, P.K. Sadhu, M.J.B. Reddy, and D.K. Mohanta, "Smart inadvertent islanding detection employing p-type μPMU for an active distribution network," IET Gen., Trans. & Dist., vol. 12, no. 20, pp. 4615-4625, 2018.

[9] S. Dutta, M.J.B. Reddy, D.K. Mohanta, M.S. Kushwah, and P.K. Sadhu, "μPMU-based intelligent island detection–the first crucial step toward enhancing grid resilience with MG," IET Smart Grid, vol. 3, no. 2, pp. 162-173, 2019.

[10] P.K. Ganivada, and P. Jena. "Active slip frequency-based islanding detection technique for grid-tied inverters," IEEE Trans. on Indust. Inform, vol.16, no.7, pp. 4615-4626, Oct. 2019.

[11] P.K. Ganivada, and P. Jena, "Pearson's correlation coefficient for islanding detection using micro-pmu measurements," IEEE Syst. Journal, vol. 15, no. 4, pp. 5078 – 5089, Sep. 2020.

[12] "Power System Monitoring Recorder", data sheet, ERLPhase Power Technologies Ltd, 2020 Available: https://www.erlphase.com/downloads/data_sheets/TESLA_4000_multi_timeframe_power_system_recorder_ds.pdf

[13] "Factors affecting PMU installation Costs", U.S. DOE-OE, U.S., Rep. Oct. 2014. Available: https://www.energy.gov/sites/prod/files/2016/10/f34/PMU-cost-study-final-10162014_1.pdf

[14] M.A. Mohamed, A.S. Al-Sumaiti, M. Krid, E.M. Awwad, and A. Kavousi-Fard, "A reliability-oriented fuzzy stochastic framework in automated distribution grids to allocate μ-PMUs," IEEE Access, vol. 7, pp. 2169-3536, 2018.

[15]M. Moradi-Sepahvand, E. Mashhour, S.S. Mortazavi, "Optimal placement of a combination of single-phase and three-phase μPMUs for observability of smart distribution networks with asymmetrical structure Mojtaba," Elect. Power and Energy Syst., vol. 105, pp. 592–601, Feb. 2019.

[16]J.R. Razo-Hernandez, I. Urbina-Salas, G. Tapia-Tinoco, J.P. Amezquita-Sanchez, M. Valtierra-Rodriguez, and D. Granados-Lieberman, "Improved performance of M-class PMUs based on a magnitude compensation model for wide frequency deviations," Mathematics, vol. 8, no. 8, p. 1361, Aug. 2020.

[17] A. K. Pradhan, A. Routray & S. R. Mohanty, "A moving sum approach for fault detection of power systems", Electric power components and systems, vol. 34:4, pp. 385-399, 2006.

[18]Rostami, Ali, Amin Jalilian, Mehrdad Tarafdar Hagh, Kashem M. Muttaqi, and Javad Olamaei. "Islanding detection of distributed generation based on rate of change of exciter voltage with circuit breaker switching strategy." IEEE Trans. on Indust. Applications 55, no. 1 (2018): 954-963.

[19]A. Rostami, A. Jalilian, S. Zabihi, J. Olamaei and E. Pouresmaeil, "Islanding detection of distributed generation based on parallel inductive impedance switching," IEEE Syst. Journal, vol. 14, no. 1, pp. 813-823, July 2019.

[20] Manual DIgSILENT PowerFactory, https://www.digsilent.de.

[21] M. E. Baran and F. F. Wu, "Network reconfiguration in distribution systems for loss reduction and load balancing", IEEE Trans. Power Del., vol. 4, no. 2, pp. 1401-1407, Apr. 1989.

[22] J. Ponoćko, "Data analytics-based demand profiling and advanced demand side management for flexible operation of sustainable power networks," Springer Theses, 2020, Available: https://doi.org/10.1007/978-3-030-39943-6.